# Advanced Reservoir Characterization of Multicyclic Carbonate Reservoirs of Bassein Formation in WO-16 area, Western Offshore Basin: A Case Study

**K.Vasudevan**

*Oil and Natural Gas Corporation Limited, India*

*62739@ongc.co.in*

## Abstract

The present study pertains to a complex, multicyclic carbonate regime on the western continental margin of India in WO-16 area. The field has an area of ~280 SKm, and has witnessed both positive and negative surprises during development drilling primarily because of patchy porosity development.

The major challenge in the area was to understand the distribution of porosity pods and establishing their continuity both spatially and temporally. Some porous pods are unconnected giving rise to patchy occurrence. To understand the porosity distribution, well, reservoir, and seismic data were integrated with sedimentological studies and image logs and calibrated with seismic attributes especially post stack P-impedance and finally a static model was developed. The model resulted in identification of exploratory and development locations for future exploitation.

Further, in this paper the Author has attempted to elucidate the complexities in Reservoir Characterization of a complex multicyclic Middle to Late Eocene carbonate reservoir of Western Offshore Basin through an innovative workflow.

## Introduction

The standard challenge of any reservoir characterization is to quantify reservoir in terms of petrophysical & reservoir properties and build a three dimensional image of the same to bring out the spatial and temporal distribution of the same.

The particular challenge becomes more difficult in case of carbonates because of different origins of porosity types, subsequent digenetic changes, spectacular variations in pore shape & size, and its uniformity/nonuniformity in distribution.

While in siliciclastic we have almost exclusively interparticle porosity, in case of carbonates it varies from interparticle to intraparticle, intercrystalline, moldic, vuggy, cavernous, fenestral and many more. This leads to high variability in effective porosity owing to different origin of pore type. Further Carbonates being chemically less stable it is susceptible to rapid dissolution and recrystallization making the job even more challenging.

Key carbonate reservoir characterization challenges are complex multi scale heterogeneity, Porosity-Permeability exhibiting little correlation and commonly mixed wet to oil wet- impacts saturation estimates, permeability and hence ultimate recovery.

To cater these uncertainties an integrated multipronged, approach covering multiple cycles from micro to meso to mega scale i.e. from SEM scale to core to seismic needs to be adopted for preparation of realistic model. (Figure 1).

## Study Area

The area under study is a wedge out prospect of carbonates formed during middle to late Eocene transgression, followed by an unconformity at the top. Basaltic basement sets the floor for sedimentation, and the carbonates onlap and wedge-out along the fringes of the basement high nonconformably (Figure 2).

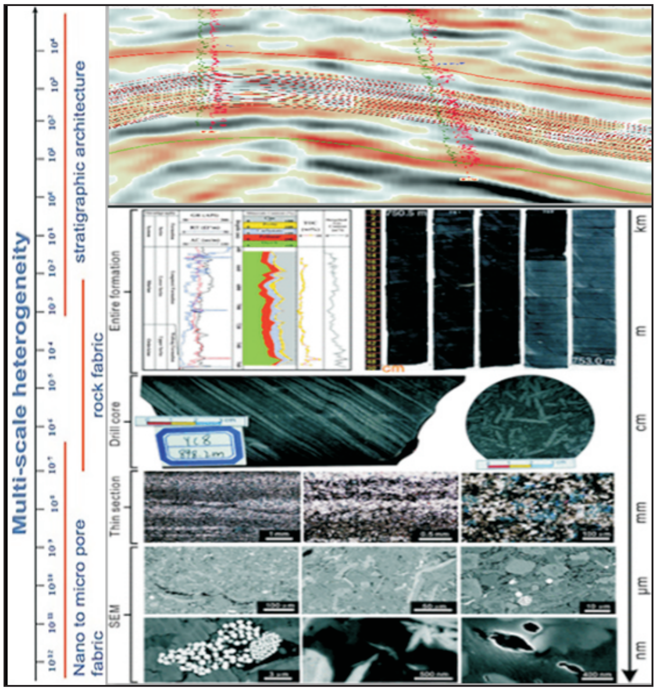

**Fig. 1:** Scale variability in carbonates from micro to mega.

## Reservoir Characterization

Carbonate rocks are significantly different from siliciclastic reservoirs due to various physic chemical process and complex diagenetic history. Therefore integration of multifaceted data from different source, vintage and process is

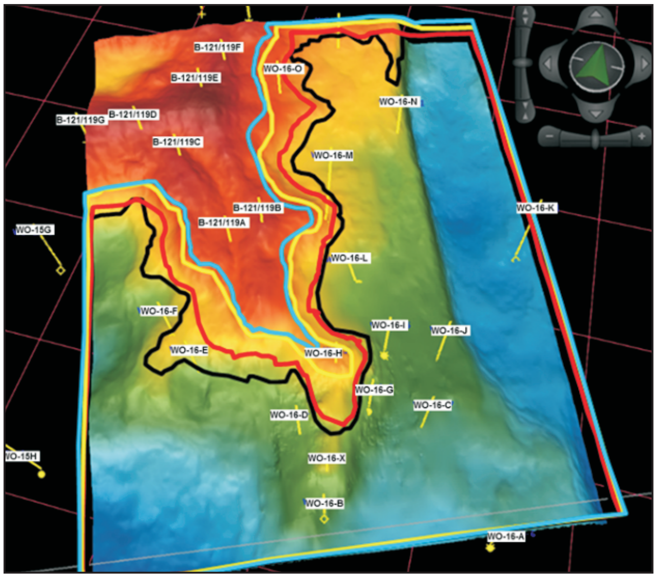

**Fig. 2:** Basement in the study area and the successive onlapping sequences of Eocene carbonates.

the utmost necessity to capture the inherent heterogeneities that beset with the carbonates.

## High Frequency Cycle Mapping

Initially correlation of stratigraphic markers from bottom to top was done on the basis of log response and bio-stratigraphic age boundaries and correlated across the area. Figure 3 stratigraphic log correlation profile among wells starting from close vicinity of wedge-out and moving away from it showing major stratigraphic markers of the study area. These markers are H5, H4 (Panna Top), Lower Bassein top, Middle bassein, H3B (Upper Bassein top) and H3A.

Bassein Formation unconformably overlies Panna formation and its thickness increases away from the wedge-out. Bassein formation in the study area is divided into three distinctly correlatable units, Lower Bassein, Middle Bassein and Upper Bassein. The transgressive Eocene Bassein carbonate sequence was divided into high frequency cycles to capture the reservoir heterogeneity and spatio-temporal variation in porosity (Figure 4).

Bassein Formation is dominantly represented by carbonate facies, with few shaly intercalations. Microfacies in the area is represented by low energy mudstone/wackestone facies in lower part to Packstone grainstone facies in the upper part (Figure 5) with a shale column at the top suggesting at the oscillating sea. Also, Biostratigraphically older succession is characterized by larger forams viz. Nummulites sp, Discocyclina sp and Fasiolites sp, while younger carbonates are characterized by smaller forams like Miliolids, Dictyoconides, sparce Coskinolina indicating shallowing of bathymetry at the depositional site, as also suggested by lithofacies variation.

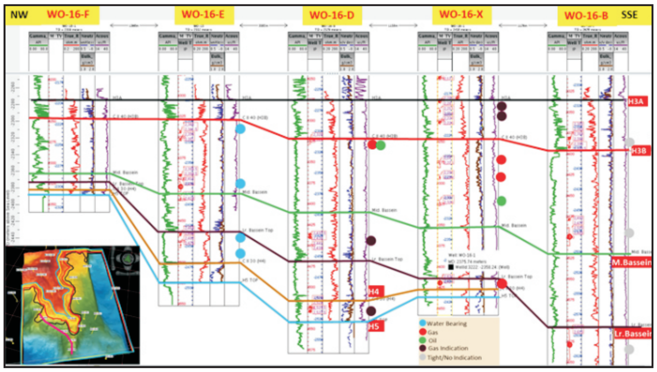

**Fig. 3:** Correlation of sequences across the study area.

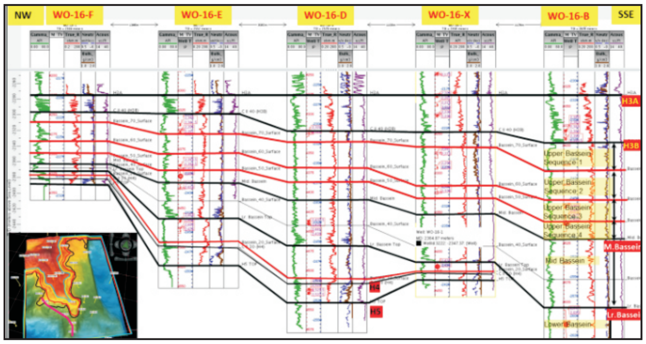

**Fig. 4:** High Frequency Cycle correlation within Bassein.

## Core-Log Integration

The primary porosity is intergranular and in the empty chambers of forams, while the secondary porosity is the forms of molds and vugs. The porosity is partially destroyed due to sparitization and deposition of argillaceous matter along the

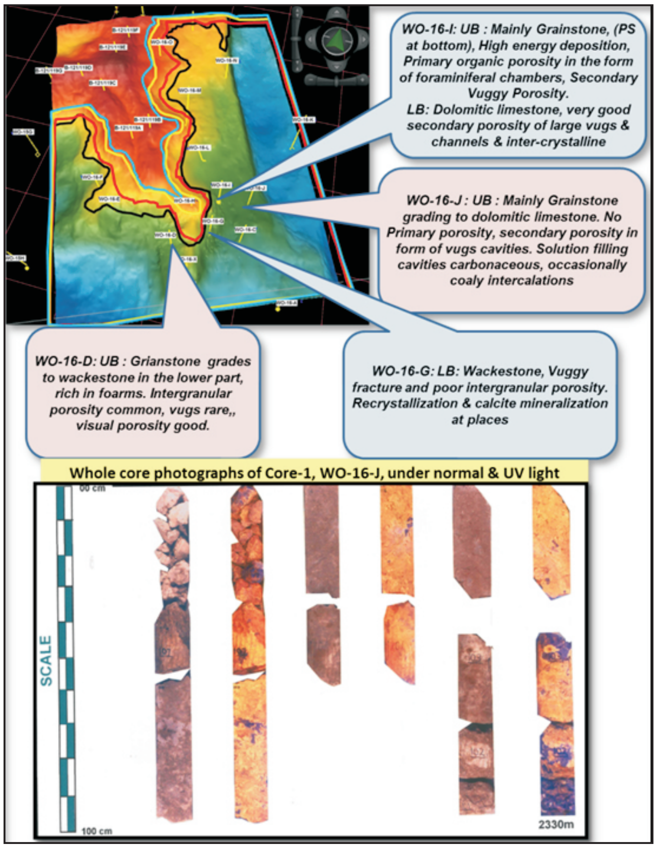
WO-16-I: UB : Mainly Grainstone, (PS at bottom), High energy deposition, Primary organic porosity in the form of foraminiferal chambers, Secondary Vuggy Porosity.
LB: Dolomitic limestone, very good secondary porosity of large vugs & channels & inter-crystalline

WO-16-J : UB : Mainly Grainstone grading to dolomitic limestone. No Primary porosity, secondary porosity in form of vugs cavities. Solution filling cavities carbonaceous, occasionally coaly intercalations

WO-16-D: UB : Grianstone grades to wackestone in the lower part, rich in foarms. Intergranular porosity common, vugs rare,, visual porosity good.

WO-16-G: LB: Wackestone, Vuggy fracture and poor intergranular porosity. Recrystallization & calcite mineralization at places

Whole core photographs of Core-1, WO-16-J, under normal & UV light

**Fig. 5:** Core megascopic studies

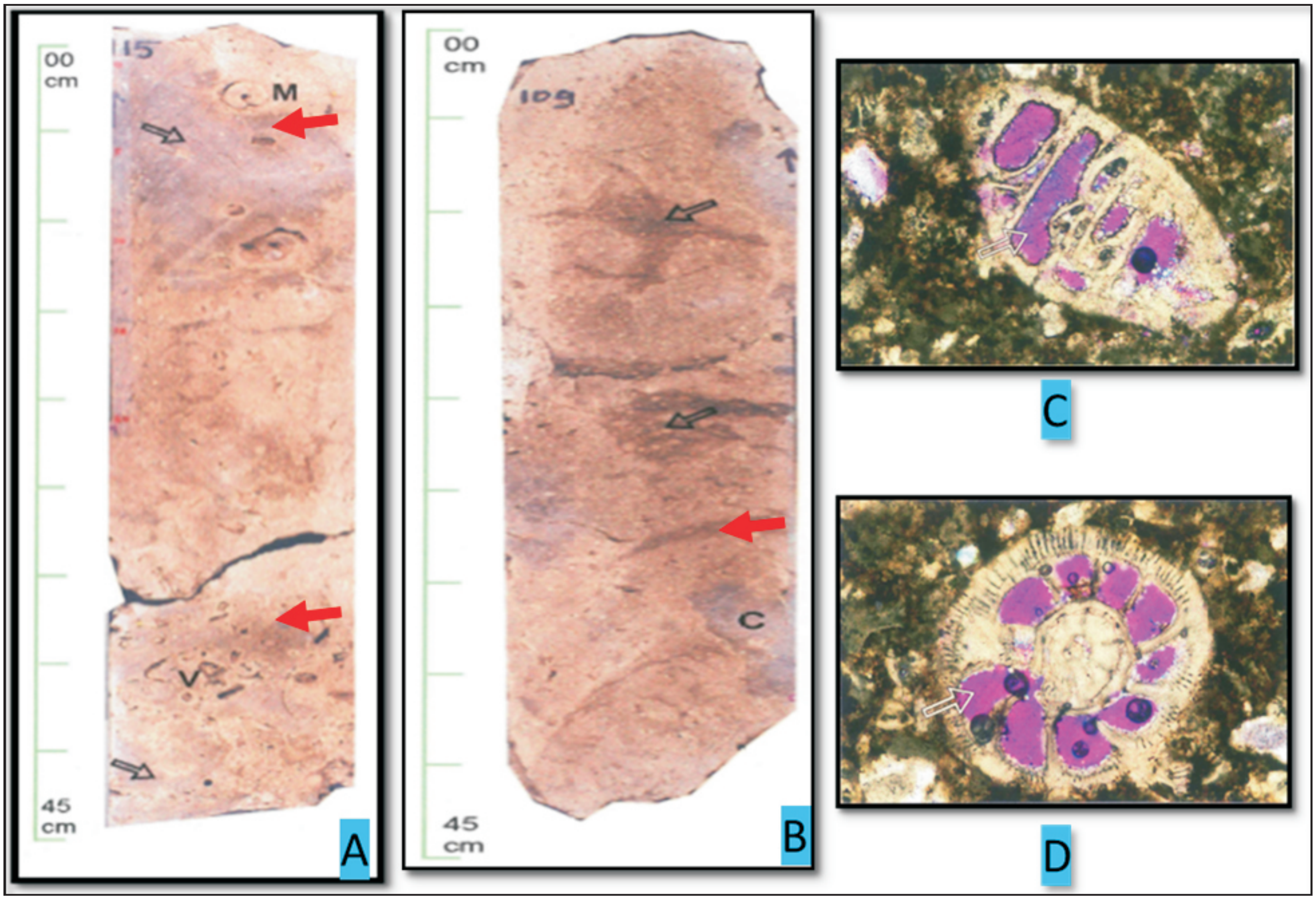

**Fig. 6:** Core Megascopy & Microscopic Studies of WO-16-J: **A.** Packstone facies exhibiting moldic porosity (M) & Solution pores/Vugs (V) The rock is partially sparitised. **B.** Accumulation of brown argillaceous matter due to solution invasion in packstone facies. **C.** Fasciolite sp exhibits good primary porosity which is partially sparitized (Longitudinal section, 90X. CN). **D.** Fasciolite sp exhibits good primary porosity (Equitorial section, 90X. CN).

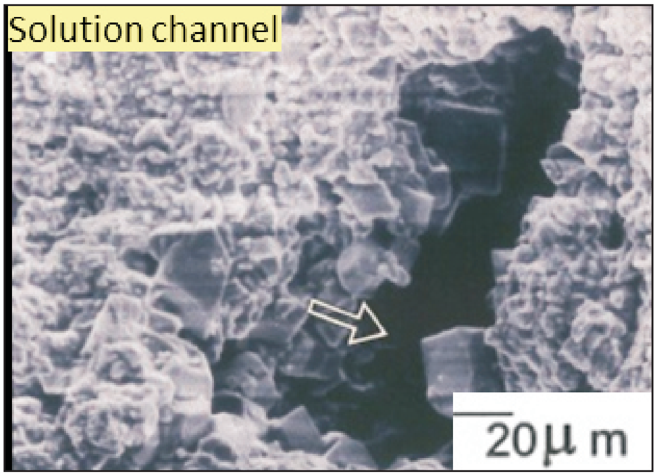

**Fig. 7:** SEM image (Upper Bassein, WO-16-J): A solution channel with longer axis of 200 µm. Partial spartitisation of micritic matrix has reduced primary intergranular porosity.

styolitic planes (Figure 6 & 7). The Cyclicity in the porosity creation and destruction is observed throughout the stratigraphic succession which is governed by lower order, high frequency sea level oscillations and the consequential hiatuses leading to exposure of geomorphic highs. To understand and illustrate this log based facies were identified and matched with core megascopic and microscopic studies. This was calibrated with the image log (Figure 8) of wells which established explicitly the cyclicity of facies and the resultant creation and subsequent destruction of porosity due

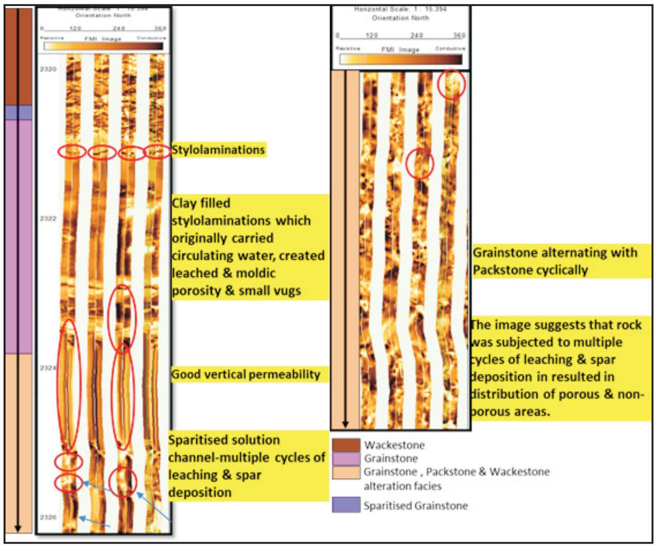

**Fig. 8:** FMI image of of WO-16-J. Cyclic alternation of low energy and high energy carbonates, multiple cycles of leaching, and alternating porous, non-porous areas.

to sparitization. This cyclicity in facies was quantified through the Fourier transform of the Gamma ray and effective porosity logs and found to be around 400 ky cycle which coincides with eccentricity of milankovichh cycle (Figure 9). The cyclicity was low during the deposition of older successions but as we move vertically in the stratigraphic column, frequency of cycles increases. This oscillation has led to minor hiatuses during the deposition of Bassein carbonates and a major hiatus at the top of it which has resulted both in creation and destruction of porosity.

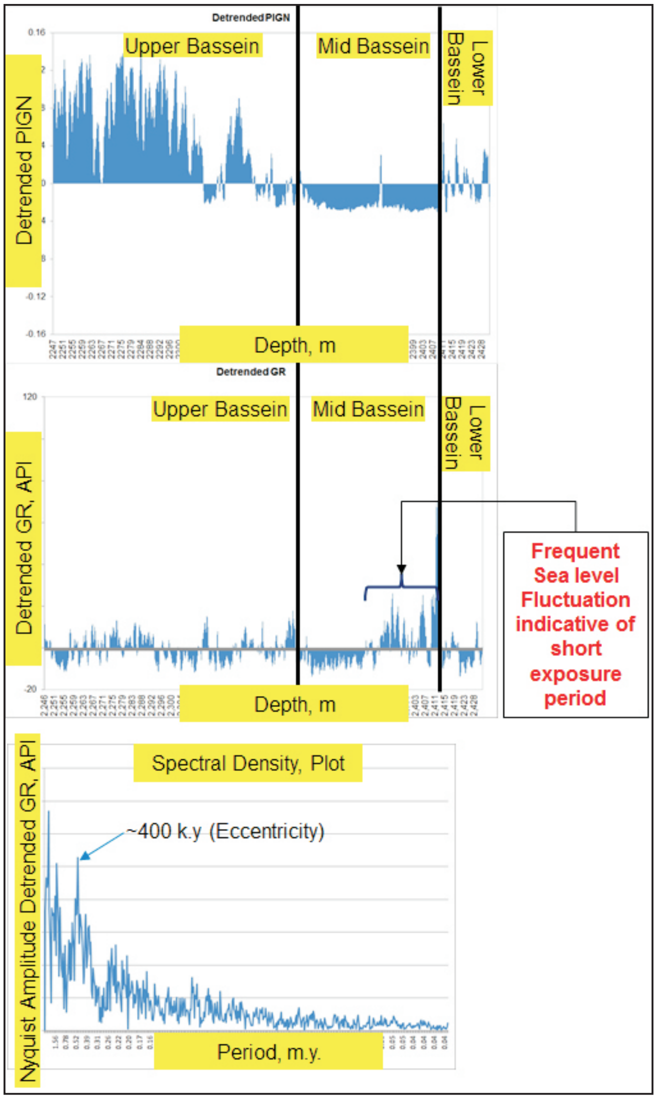

**Fig. 9:** Effect of Eccentricity in GR cycle

## Seismic Inversion

Lab measurements have indicated that the velocity in the area is affected by presence/absence of porosity and since P wave velocity and bulk density are interrelated, post stack inversion was carried out to understand the spatial distribution of the porosity pods (Figure 10).

Good match was observed between inverted and log impedance. Cross plots of Effective Porosity and P-Impedance reveals that the impedance has inverse linear relationship with porosity in the study area (Figure 11). Lower

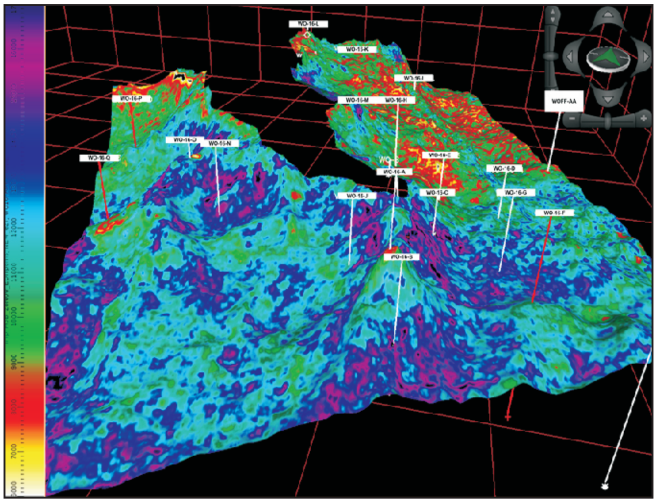

**Fig. 10:** P-Impedance slice of H3B±8ms draped over structure on top of H3B showing extent of porous pods

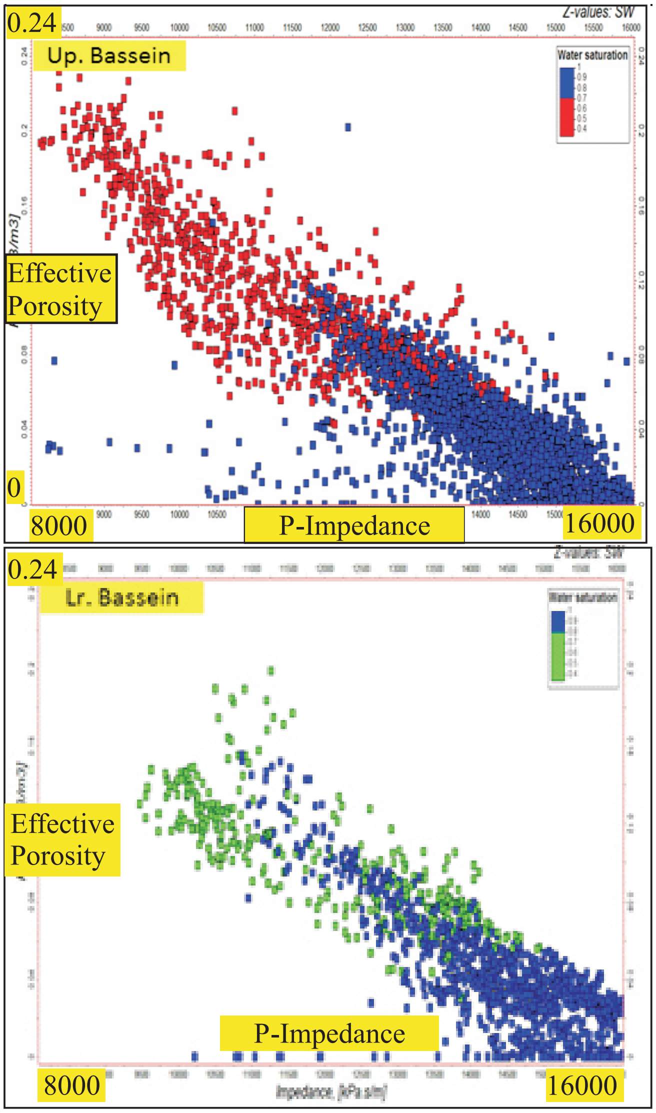

**Fig. 11:** Cross plots between P-impedance vs Effective porosity shows an inverse relationship between P-Impedance and porosity.

impedance range corresponds to better porosity areas in clean carbonate country. The tight carbonates show impedance of more than 13000 KPa.s/m. whereas porous carbonates show impedance in the range of 8800 to 12400 KPa.s/m for Upper Bassein unit, while for the Lower Bassein, it ranges 10500 to 13500 KPa.s/m

Not only the porous pods but formation fluid types also get distinguished on the basis of impedance. Free Gas and Gas cap Gas bearing formation shows impedance range variation from 8500 KPa.s/m to maximum 12000 KPa.s/m whereas in oil bearing formation it extends from 9500 KPa.s/m to maximum 13500 KPa.s/m.

Initially the extent of porosity pods associated with specific fluid type was demarcated in the well. Later, on the basis of pressure data, hydro-dynamically connected porosity patches were correlated within the field. These connected porous bodies acted as speed zones within which fluid can move freely.

## Porosity Model

Porosity model was generated keeping impedance volume as the secondary trend and well based porosity as primary constraint. Porosity model was conditioned to seismic data using colocated co-krigging. Gaussian Random Function Simulation (GRFS) using collocated co-krigging was performed taking P-Impedance as the secondary variable. Flow chart for preparation of effective porosity volume is placed at Figure 12.

For the propagation of effective porosity initially the Probability Density Function (PDF) observed in the well logs (Figure 13) were given priority. Effective Porosity volume generated through this process was skewed towards lower porosity. Average effective porosity maps generated for Upper Bassein section, which is good producer throughout the field (Figure 14), shows abundance of tight patches and could not explain the production behavior of development wells due to inadequate well samples. PDF of effective porosity of logs at well level is more representative of vertical distribution of effective porosity in the well. In the next stage the propagation of effective porosity in the model is biased with the PDF of seismic P-Impedance (Figure 14) since P-Impedance represents inter-well space more aptly than the scattered well control.

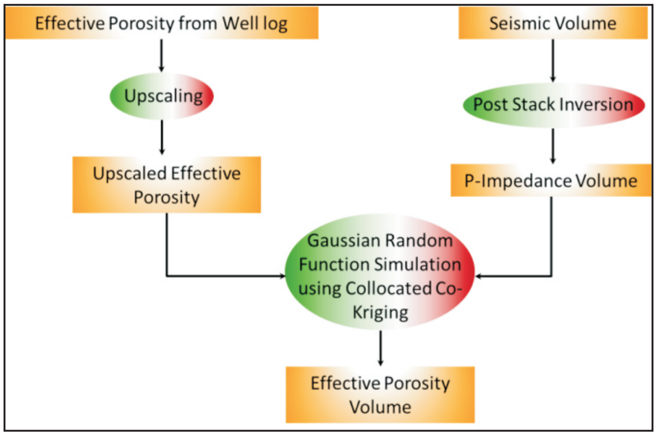

**Fig. 12:** Flow chart for Effective Porosity Volume

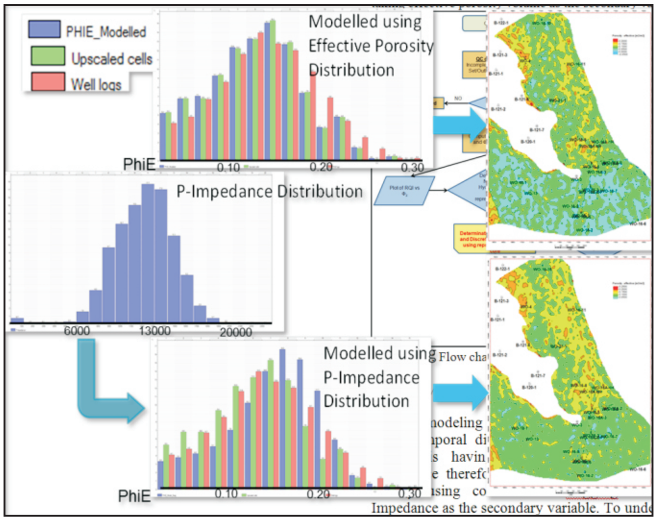

**Fig. 13:** Probability Density Function of Effective Porosity observed in the well logs and P-Impedance volume vis-à-vis modelled Effective Porosity

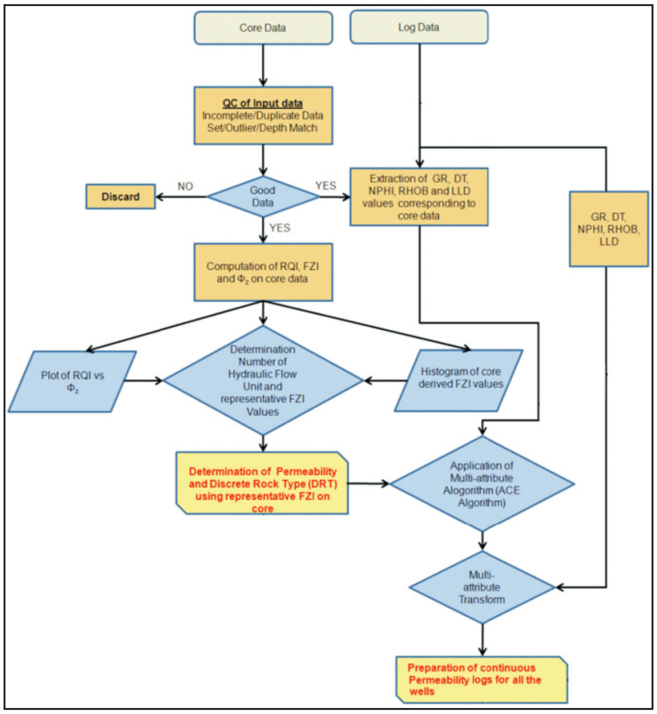

**Fig. 14:** Flow chart for calculating permeability

## Permeability Model

Pore throat radius is the prime element that controls the initial/residual hydrocarbon distribution and fluid flow. Existence of hydraulic units or petro-physically distinct zones with similar fluid flow characteristics is defined by the variation in pore geometry attributes.

First Hydraulic flow units were identified based on core porosity and permeability data, followed by permeability calculation and rock type discretization in cores and population of permeability and rock type discretization in all the uncored sections/logs using multi attribute transform. Clustering algorithm (histogram analysis) was applied to find the median and extent of flow parameters in each flow units. Flow chart for the calculation of permeability is placed in Figure 14. For the population of permeability in the model permeability data was conditioned to effective porosity model using collocated co-krigging. Gaussian Random Function Simulation (GRFS) using Collocated co-krigging was performed taking effective porosity volume as the secondary variable.

## Density Model

Density modeling was taken up to understand the spatio-temporal distribution of dolomitization. As density is having linear relationship with P-Impedance therefore it would allow to propagate density using collocated co-krigging taking P-Impedance as the secondary variable. To understand the effect of dolomitization series of density simulation were carried out by changing the percentage volume of calcite-dolomite in the system with predefined porosity, water and gas saturation.

This exercise lead to restrict the upper density limit of calcite effect up to 2.68 gm/cc and lower limit being 2.4 gm/cc (considering 15% being the close to average porosity and that will be filled with gas). Applying this cut off calcite-dolomite model had been prepared. 3D perspective of calcite dolomite model has been placed in Figure 15. It is evident that effect of dolomitization has increased Middle Bassein downward. Incorporating this observation a Conceptual Diagenetic Model has been prepared (Figure 16) to capture the porosity evolution of Bassein Formation in WO-16 field.

## Diagenetic Model

Vadose zone diagenesis along the exposed geomorphic highs led to porosity generation while porosity destruction is attributed to diagenesis in phreatic zone along the low axis (Figure 10). During Paleocene-early Eocene Panna clastics were deposited over basement making the country rock for the carbonate deposition. Rising sea level, scarcity of clastic input, greenhouse climatic condition etc favoured the carbonate deposition and Lower Bassein Carbonate Formation deposited over Panna Formation. Towards the Basement high Lower Bassein Carbonate Formation lies non-conformably over Basement, ultimately forming wedge out structure. After Lower Bassein Carbonate deposition sea level dropped exposing part of the carbonate over the basement highs. These carbonates were exposed to weathering and underwent diagenesis in vadose and meteoric realm leading to karstification at the structural highs. Due to lowering of sea level restricted marine environment would prevail in sags between two adjacent highs. In the restricted marine environment due to evaporation hyper saline environment lead to dolomitization and destruction of porosity. Following this Middle and Lower Bassein Carbonate Formation deposited due to cyclic rise of sea level and lowering of sea level lead to karstification at the structurally higher places. Middle Basein karstification due to lower exposure time partially filled up the already karstified pores of Lower Bassein Formation due to leaching. Pronounced unconformity at the H3B lead to very long exposure at the Upper Bassein time and that completely filled up the pores of Middle Bassein karstified portion leading to destruction of porosity.

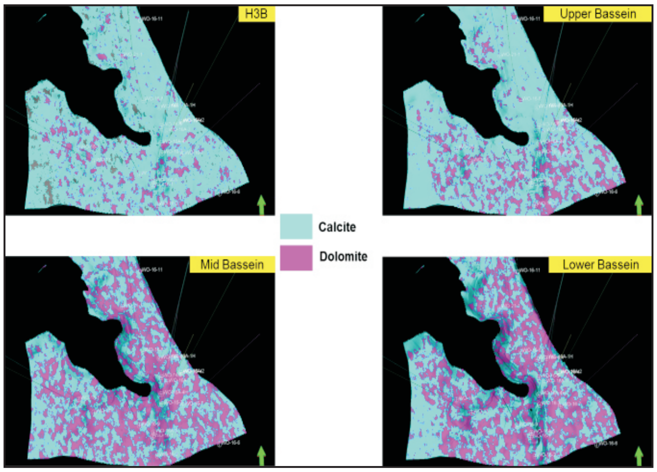

**Fig. 15:** 3D perspective view of Calcite and Dolomite model

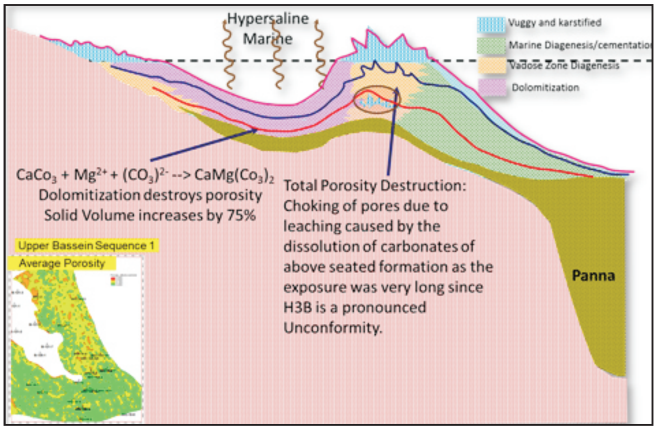

**Fig. 16:** Diagenetic Model: Cyclic Porosity creation and destruction during vadose & phreatic zone diagenesis respectively

## Conclusion

Integration of multidisciplinary and multi scale data lead to identification depositional environment, diagenetic history and sweet spots in the Bassein formation in WO-16 field.

Fluctuating sea level, change in the bathymetry and broad depositional setting was brought out by integrating the core micrograph, core megascopy, biostratigrahic data and FMI logs.

Shallow marine carbonates of Bassein Formation underwent different diagenetic episodes due to the underlying basement architecture. Carbonates sitting on the open marine underwent marine cementation and marine digenesis depending on the position of Calcite/Aragonite lysocline. In the restricted marine environment between two adjacent high dolomitization destroyed the porosity and in the basement highs porosity created due to karstification but Middle and Lower Bassein karstified layers got filled up due to leaching activity. These proposition was further validated by analysis of core micrograph where the calcite cementation showed fibrous growth around the bioclast and comparison of detrended Gamma Ray vs effective Porosity curves.

This study lead to understand that Upper Bassein is mostly Structural Play and that of Lower Bassein is Strati-Structural.

Incorporation of porosity, permeability, density and diagenetic model lead to identification of three exploratory location and nine development location for the further exploitation of Bassein hydrocarbon.

## Acknowledgement

The author expresses his sincere gratitude to Sh. A.K. Dwivedi, Director (E), ONGC for permission to publish this paper. The author thankful to Dr. Harilal, GGM-Head INTEG and Shri Ashutosh Bhardwaj, ED-HOI, GEOPIC, ONGC for their constant guidance and support.

The author would like to thankfully acknowledge the technical contribution and scrutiny of manuscript of this paper by Sh. Aninda Ghosh, Dy SE (Reservior), ONGC.

### Referrences

Sedimentological studies and Integration of FMI and NMR logs with cores: Well No. WO-16-9, RGL, MRBC, ONGC Ltd., June 2000.